Energy and damping analysis of the wet-modes of an elastic floating structure

D. Dessi
INSEAN- Italian Ship Model Basin, Rome, Italy

ABSTRACT

In this paper, the bending modes of an elastically scaled segmented hull model are identified using the proper orthogonal (or Karkunen-Loeve) decomposition. Despite the conceptual simplicity of the method, its application to floating structures requires some cares and motivated the analysis of two sets of data, accelerations and strains, with two different tailoring of the original method, that allows to provide information about both the damping and the energy distribution among the identified modes.

INTRODUCTION

Structural dynamics has been covering in last decades new topics, encouraging applications that in the past missed proper theoretical support. The identification of ship vibration modes, objective of the present work, is one of the problems in ship engineering benefiting of recent theoretical achievements in structural dynamics. The advantages of identifying modal parameters by performing modal tests using the ambient excitation and measuring only the responses of the structure, *i.e.*, ambient or operational conditions, made the output–only modal testing very popular [1] in recent years. In fact, the test procedure consists only in measuring the response of the system, resulting then an easier way for characterizing the dynamic behavior of the structure with respect to the traditional experimental modal analysis. Furthermore, with this approach, it is possible to identify the dynamic properties of the system in real operative conditions where the loading conditions are, in general, unknown or substantially different from those simulated in modal tests. In this paper a time-domain procedure to identify the vibration modes of a floating structures, based on the analysis of both displacements and accelerations, is presented. The implemented time-domain technique is the proper orthogonal decomposition (POD) that provides the functional basis that accounts for more captured energy than any other orthogonal one. The POD has been applied in its straightforward formulation and in a slightly different version as well, named band-pass POD, that exploits preliminary filtering around resonant peaks of the analyzed signals to enhance the convergence of the proper orthogonal modes (POMs) to the linear normal modes (LNM) in case of poor information about the mass distribution. The presented procedure has been employed to analyze the experimental data provided by accelerometers and strain-gages applied to the flexible backbone of an elastically scaled segmented-hull model sailing in both irregular sea and regular waves in the towing-tank. The comparison between the modes shapes identified with the two different procedures (original POD on the displacements and band-pass POD on the accelerations) allows to show the effectiveness of this method and the possibilities and limitations related to the use of each procedure. Some results related to the present application, like energy ordering of the wet-modes and its dependence on the encountered sea pattern, as well as the modal damping variation with ship forward speed, are discussed in the paper, disclosing the POD capability to provide new insights in the analysis of hydroelastic phenomena.

IDENTIFICATION TECHNIQUE

The proper orthogonal decomposition, often called Karhunen-Loeve decomposition from the name of the authors that stated the method (see Karhunen [2] and Loeve), has appeared in the scientific literature with various names depending on the area of application (statistics, oceanography and meteorology, psychology and economics), until the method was successfully applied in fluid dynamics when computational costs has dropped (see, e.g., Lumley [3]). The first applications of the proper orthogonal decomposition in the field of structural dynamics date back to the nineties and were mainly devoted to nonlinear problems. For an extended review about the use of proper orthogonal decomposition for dynamical characterization and order reduction of mechanical systems, it is possible to refer to Kerschen *et al.* [4]. In the field of structural dynamics of linear systems, several papers treated the relationship between the proper orthogonal modes and the linear normal modes. Feeny and Kappagantu [5] proved the convergence of the proper orthogonal modes to the linear normal modes for discrete systems in the case of undamped free vibration. Later, Feeny and his co-authors extended the treatment to the case of continuous systems and to the case of randomly excited systems. From all these works emerged that the proper orthogonal decomposition can be a promising alternative to traditional input-output modal analysis methods.

Consider a scalar random field $w(x,t)$ with zero mean, defined on a spatial domain Ω. It can be expressed in the variables-separated form as an infinite sum of contributes

$$w(x,t) = \sum_{k=1}^{\infty} w_k(t)\psi_k(x), \tag{1}$$

or, on the other hand, it can be conveniently approximated using only a limited number L of terms. For instance, in the present application, $w(x,t)$ is the displacement field that satisfies the equations

$$\mu(x)\ddot{w}(x,t) + \mathcal{L}_1 w(x,t) = f(x,t), \tag{2}$$

where $\mathcal{L}_1$ defines a linear self adjoint operator (with respect to given boundary conditions), $\mu(x)$ is the mass per unit length and $f(x)$ is the forcing term. Clearly the expansion provided by Eq. 1 is not unique and depends on the choice of the basis functions $\psi_k(x)$ (Fourier series, Chebychev polynomials and so on). The proper orthogonal decomposition deals with one possible choice of the functions $\psi_k(x)$, based on the criteria of orthogonality between the basis functions and optimality in the least squares sense: fixed a limited number L of functions, they provide an approximated representation of the field that accounts for more energy compared with any other orthogonal function representation.

Skipping about the continuous formulation of the problem in terms of eigenfunction of a properly defined integral operator, for lack of conciseness it is implicitly assumed that the proper orthogonal modes can be equivalently determined by applying the proper orthogonal decomposition on the solution $\mathbf{w}(t)$ of the following equation

$$\mathbf{M}\ddot{\mathbf{w}} + \mathbf{K}\mathbf{w} = \mathbf{f}, \tag{3}$$

that represents a suitable discretization of the continuous problem defined by Eq. 2. Thus, we intend to search for the decomposition $\mathbf{w}(t) = \sum_{k=1}^{L} w_k(t)\mathbf{p}_k$ that gives the best representation of the solution $\mathbf{w}$ in the sense already specified for the continuous problem, where the vectors $\mathbf{p}_k$ are the proper orthogonal modes. At this point, it is useful to introduce the following transformation in Eq. 3, $\mathbf{w} = \mathbf{M}^{-1/2}\hat{\mathbf{w}}$, thus obtaining $\ddot{\hat{\mathbf{w}}} + \mathbf{M}^{-1/2}\mathbf{K}\mathbf{M}^{-1/2}\hat{\mathbf{w}} = \mathbf{M}^{-1/2}\mathbf{f}$, that can be recast finally as

$$\ddot{\hat{\mathbf{w}}} + \hat{\mathbf{K}}\hat{\mathbf{w}} = \hat{\mathbf{f}}, \tag{4}$$

where the matrix $\hat{\mathbf{K}}$ is still symmetric. Equation 4 defines an undamped mechanical system with uniform mass distribution ($\mathbf{M} = \mathbf{I}$ in this particular case) for which the linear normal modes are directly provided by the proper orthogonal decomposition. The M components of the vector $\hat{\mathbf{w}}(t) = \{\hat{w}_1(t), \ldots, \hat{w}_m(t), \ldots, \hat{w}_M(t)\}^T$ represent the transformed displacements in the same points where, for instance, the measurements were performed. If N 'observations' for each of the M components of the vector $\hat{\mathbf{w}}$ are available, let us define a new vector variable, $\hat{\mathbf{w}}^{(m)} = \{\hat{w}_m(t_1), \ldots, \hat{w}_m(t_N)\}^T$, that is the sampled time history relative to the generic component $\hat{w}_m(t)$ of the state space vector $\hat{\mathbf{w}}(t)$, assuming that the mean value was previously subtracted. Thus, the $N \times M$ response ensemble matrix is constructed as

$$\hat{\mathbf{W}} = [\hat{\mathbf{w}}^{(1)}, \hat{\mathbf{w}}^{(2)}, \ldots, \hat{\mathbf{w}}^{(M)}], \tag{5}$$

that allows to obtain the sample covariance matrix as

$$\mathbf{R}_{\hat{W}} = (1/N)\hat{\mathbf{W}}^T \cdot \hat{\mathbf{W}}, \tag{6}$$

where the symbol $\cdot$ denotes the inner product. Considering the system response in its continuous form (Eq. 2), it emerges that the averaged auto-correlation function $R(x, y)$ has been replaced by the $M \times M$ sample covariance matrix $\mathbf{R}_{\hat{W}}$. The proper orthogonal modes are calculated as the eigenvectors of the covariance matrix $\mathbf{R}_{\hat{W}}$, *i.e.*,

$$\mathbf{R}_{\hat{W}}\hat{\mathbf{p}} = \sigma\hat{\mathbf{p}}, \tag{7}$$

where σ is the corresponding proper orthogonal value. The proper orthogonal values give an indication of the level of excitation of the correspondent proper orthogonal mode. In fact, if $\mathcal{E}$ is the energy associated to the random field, it can be expressed as

$$\mathcal{E} \propto \sum_{i=1}^{M} \sigma_i, \tag{8}$$

and the relative energy captured by the k-th proper orthogonal mode is $\varepsilon_k = \sigma_k/\mathcal{E}$. It is worth to remark that energy is defined as the norm of the signal and not as mechanical energy.
Defining the $M \times M$ eigenvector matrix $\mathbf{P} = [\hat{\mathbf{p}}_1, \hat{\mathbf{p}}_2, \ldots, \hat{\mathbf{p}}_M]$, it follows that the values of the proper orthogonal coordinate (POC) a_k at the different time instants t_n is represented by the columns of the $N \times M$ matrix $\mathbf{A} = [\mathbf{a}^{(1)}, \mathbf{a}^{(2)}, \ldots, \mathbf{a}^{(M)}]$ given by

$$\mathbf{A} = \mathbf{W} \cdot \hat{\mathbf{P}} \tag{9}$$

with $\mathbf{a}^{(k)} = \{a_k(t_1), \ldots, a_k(t_N)\}^T$. Thus, one finally obtains, by suitable interpolation over the proper coordinate vector $\mathbf{a}^{(k)}$,

$$\hat{\mathbf{w}}(t) = \sum_{k=1}^{L} a_k(t)\,\hat{\mathbf{p}}_k, \tag{10}$$

that is the discretised form of Eq. 1, where, in general, $L \leq M$, *i.e.*, the number of assumed modes is less or equal than the number of measurement points. This procedure to compute the proper orthogonal decomposition is more efficient with respect to the snapshot method (see Lumley [3]) from a computational point of view when the number of time instants N is larger than the number of measurements points M.

MODEL DESCRIPTION

In the present case, the segmented model technique with an elastic backbone (rectangular, hollow and made of an aluminium alloy was built with 20 elements of constant stiffness and shear area) was adopted in order to scale the bending stiffness of the fast ferry Fincantieri *MDV3000* (for more details, refer to [6]). Each segment is connected to the elastic beam with short legs and the gaps between adjacent segments are made water-tight by using rubber straps (Fig. 1). The short legs were built by using steel, whereas the hull segments are of fiber-glass. The materials employed in the model construction were chosen for several technological reasons; among them, the limitation of the total weight was one of the main concerns. Thus, the model-scale was set equal to $\lambda = 1/30$, whereas the number of segments was set to six.

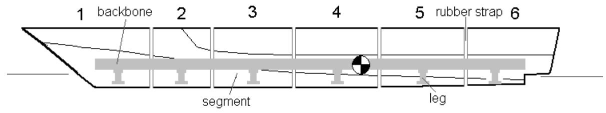

Fig. 1 Sketch of the segmented model.

EXPERIMENTAL INVESTIGATION

Analysis of strain-gauge signals

The identification procedure that makes use of the strain-gage signals exploits the time-histories of the vertical bending moment relative to each measurement point. Accordingly to the Euler-Bernouilli beam model, the elastic displacement is given by

$$w^{(e)}(x, t) = c_1 + c_2 x + \int_{-\ell_1}^{x} \left[\int_{-\ell_1}^{x_2} \frac{M_y(x_1, t)}{EI_{yy}(x_1)}\, dx_1 \right] dx_2, \tag{11}$$

with EI_{yy} the bending rigidity, where E is the Young modulus, $I_{yy}(x)$ is the sectional moment of inertia with respect to the y axis, $\ell_1 > 0$ is the absolute distance of the center of gravity from the beam end. The presence of the constants of integration, due to the free-end boundary conditions of the floating beam, indicates that the elastic mode shapes may appear arbitrarily translated and rotated, depending on the choice of the constants c_i (note that they can be even time-dependent). To avoid this trouble, the total displacement $w(x, t)$ instead of $w^{(e)}(x, t)$ is then processed with the POD. In fact, due to the orthogonality relationships between the proper orthogonal modes, the elastic modes ($j = 3, \ldots$) has to be orthogonal to the rigid-body modes ($i = 1, 2$) and this condition implies the correct translation and rotation of the mode shapes.
It is important to recall that information about the mass distribution is needed to get the POMs converging to the LNMs. This requirement would be unnecessary if the input signals were preliminary filtered so as to leave just a single mode contribution. However, the number of measurement points ($M = 12$) is large enough to build a sufficiently accurate mass matrix and, avoiding filtering, the energy distribution among modes can be retrieved. The added mass of the segment has to be taken into account too and was calculated numerically by integrating along the segments the distribution of the sectional added mass provided by the Lewis' infinite-frequency approximation. In Figs. 2, 3 and 4 the identified proper orthogonal modes are plotted for the case $Fr = 0.44$ and an irregular sea with a Jonswap spectrum, being $H_s = 2\,m$ and $T_s = 7.5\,s$ the correspondent significant wave height and period, respectively, at full-scale. It is worth to note that the chosen parameters

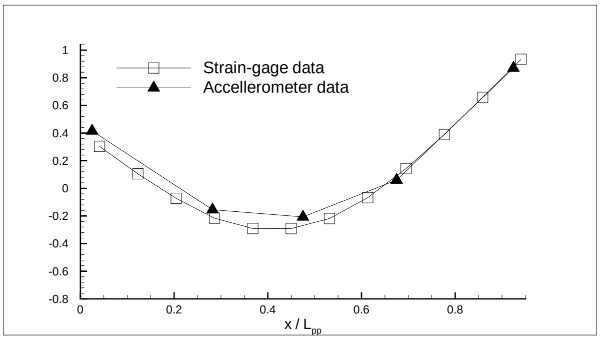

Fig. 2 Identified 2-nodes POM at $Fr = 0.44$.

λ_w/L_{pp}	$\bar{\sigma}_1$	$\bar{\sigma}_2$	$\bar{\sigma}_3$	$\bar{\sigma}_4$
0.60	97.15728	2.80306	0.03866	0.00085
1.35	98.76840	1.21798	0.01307	0.00051
1.75	99.75023	0.23354	0.01549	0.00063
2.30	99.80793	0.17368	0.01626	0.00192
irr. sea	$\bar{\sigma}_1$	$\bar{\sigma}_2$	$\bar{\sigma}_3$	$\bar{\sigma}_4$
with slams	98.7682	1.2076	0.0227	0.0012
w/o slams	98.9233	1.0545	0.0206	0.0013

Table 1 POV percentage calculated on the elastic modes for different encountered seas ($Fr = 0.44$).

for the sea do not cause any large amplitude motion for the scaled ship. Each identified mode is compared with that one calculated via modal analysis carried out on a finite element model relative to the complete backbone model. From the observation of these figures it emerges that the differences between the computed and experimentally identified modes are significative only for the 4-nodes mode.

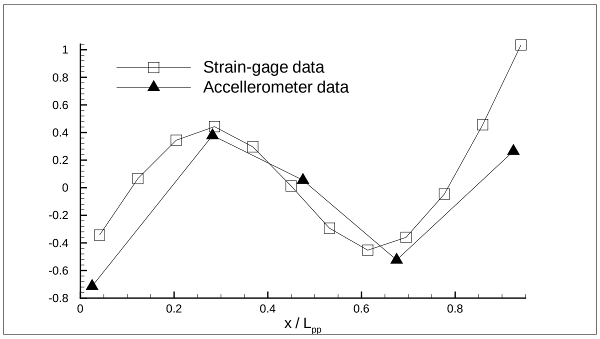

Fig. 3 Identified 3-nodes POM at $Fr = 0.44$.

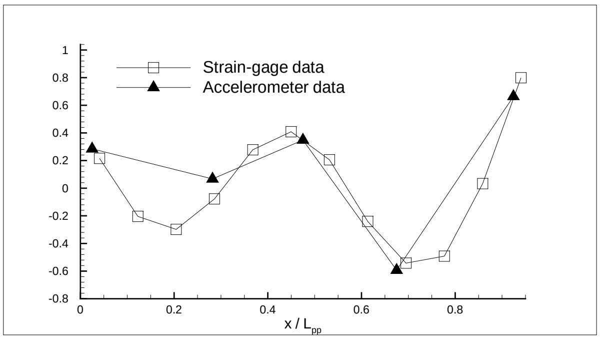

Fig. 4 Identified 4-nodes POM at $Fr = 0.44$.

The POMs do not present any apparent variation in shape if the encountered sea changes its main spectrum parameter (significant wave height and period) or if the ship sails through regular waves. In fact, a POM variation can occur only if the system hydrodynamic coefficient (principally the added mass and damping) be affected by the different (but physically admissible) seaways encountered by the ship. However, since the wave elevation is a zero-mean process, it follows that despite the nonlinear relationship relating the hydrodynamic coefficients to the wave elevation, the average of their perturbation is close to zero and POD is not sensitive to this small coefficients fluctuations, thus not providing any clear POM shape alteration. On the other hand, the level of excitation of each identified mode may significantly change from one mode to the other, as it will be shown in the following. Considering as a starting point the sea state already considered for the identification of the POM shapes ($H_1/3 = 2\,m$ and $T_1 = 7.5\,s$), in Fig. 5 the proper orthogonal values are represented for all the modes (i.e., rigid-body and elastic modes), using a logarithmic scale on the y-axis, highlighting the different energy content associated to each identified mode. It is evident that the first bending mode (2-nodes mode) is highly predominant on the others bending modes, as confirmed also by the analysis of the correspondent POC time-history.

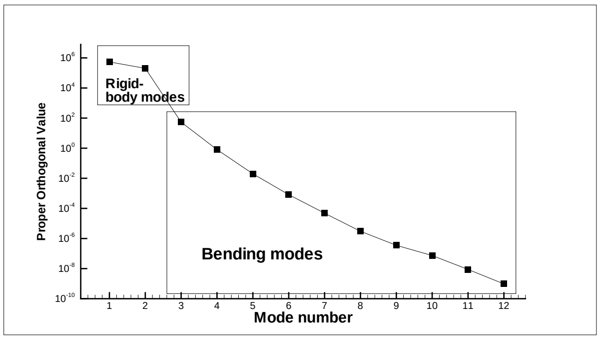

Fig. 5 POVs spectrum (irreg. sea).

It has been shown that regular waves, despite of their apparent sinusoidal wave form, do not determine a monochromatic load excitation at all and the resulting load spectrum amplitudes, in the frequency range of the vertical bending modes, vary barely so as to excite rather uniformly all the vibration modes. Therefore, it is not surprising that the vertical bending modes can be identified in regular waves as well, via the POMs converging to the corresponding LNM. However, the POVs appear more sensitive to the excitation features, as it appears from the results shown in Tab. 1, where the percentage of energy for each elastic mode $\bar{\sigma}_i$ is calculated with respect to the overall 'elastic' energy alone (more precisely, to the summation of the energy associated to the computed bending modes), *i.e.*, $\bar{\sigma}_i = \sigma_i / \sum_{j=3}^{M} \sigma_j$. The trends provided by Tab. 1 show the tendency of the first elastic POV to increase with the wave length and, on the opposite, a rather negative slope for the second POV (further considerations for the subsequent modes may be affected by low excitation levels). These trends can be explained recalling the general form of the response of a linear structural system to external excitation, since hydroelastic coupling for the bending modes is low. Thus, the role of the load projection upon the bending modes is much more relevant in amplifying the response than the possible resonance effect due to the load spectrum. It seems reasonable to observe that, as expected, if λ_w/L_{pp} is close to 1, the waveform is close to the shape of the second bending mode (higher value of the 2^{nd} POV), whereas if $\lambda_w/L_{pp} \to 2$, the waveform resembles more to the 1^{st} mode. Returning back to the irregular sea case, there is not any clearly predominant wave length but, anyway, the prevalence of certain wavelengths around the peak of the sea energy spectrum enhances the response of the two-node bending mode. It is interesting, in this case, to evaluate the effect of slamming events on the modal response. For the same towing-tank run, two time-histories of the same duration, one including slamming events and a second one without slamming events, were isolated for the case $H_1/3 = 5\,m$ and $T_1 = 6\,s$, with $Fr = 0.44$. The identification of the occurrence of slamming impacts were done by using the wavelet transform of the midship VBM to highlight the presence of two-mode vibrations originated from each slamming event (whipping). Comparing their POV spectrum, as shown in Tab. 1, a slight decrease of about 1% in the two-node mode energy appears, caused by the presence of impulsive loading associated to slamming events. Though, as expected, impulsive (or, at least, short period) loading seems to emphasize the contribution of higher modes, the differences remain mild also if other time records are compared to each other.

Analysis of accelerations

Accelerations can be processed by the proper orthogonal decomposition, providing directly proper orthogonal modes that do not differ from those obtained using displacements (only normalization constants may not be the same). The accelerations can be expressed as:

$$\ddot{w}(x,t) = \ddot{w}_G(t)\phi_1(x) + \ddot{\theta}(t)\phi_2(x) + \sum_{i=3}^{N} \ddot{w}_i(t)\phi_i(x) \quad (12)$$

where the mode shapes are those already defined for the displacements if the system is supposed to be linear.

On the other hand, the acceleration data-set considered in the present work constitutes a typical example of a low spatial sampling because there are only 5 measurement points. For this reason, it is convenient to apply the proper orthogonal decomposition to the filtered time histories because this prevents to provide any information on the mass distribution, that, in this case, would be too approximate to ensure convergence of the POMs to the LNMs. The preliminary step is in this case to select the frequency peak corresponding to the sought after mode in the auto-spectral density functions relative to each acceleration signal. Assuming a single degree of freedom hypothesis, a $5-th$ order Butterworth band-pass filter around the selected frequencies was used, adjusting the low and high cut-off frequencies according to the local trend of the spectrum. Thus, for each sought after mode, the time-histories of the five accelerometers were first filtered with he corresponding cut-off frequencies and then processed by the POD algorithm. It is worth to note that, since only one mode at time is present, no orthogonality relationship between the modes can be satisfied. This implies that also those global modes affected by the local leg modes may appear this time. Therefore, one 2-nodes mode ($f_n = 7.3Hz$), one 4-nodes mode ($f_n = 34.7Hz$) and five 3-nodes modes were identified. In order to select which of the identified 3-nodes is candidate to represent better the main beam modes, the Modal Assurance Criterion index between the five 3-nodes modes and the remaining 2-nodes and 4-nodes modes needed to be calculated. The results of this computation are reported in Tab. 2 indicating that the 3-nodes mode with $f_n = 22.3Hz$ satisfies better the orthogonal condition, *i.e.*, $AutoMAC \simeq 0$, with respect to both the 2-nodes and 4-nodes global modes (note the underlined numbers in Tab. 2). Then, the identified modes most representative of the global bending behaviors of the system are plotted in Figs. 2, 3 and 4 respectively. For sake of comparison, also the proper orthogonal modes identified on the basis of displacements have been reported.

$i-th$ mode	$f_n i[Hz]$	MAC $(i,1)$	MAC $(i,7)$
2	13.0	0.467	0.341
3	14.1	0.157	0.090
4	16.2	0.612	0.566
5	22.3	<u>0.002</u>	<u>0.005</u>
6	29.0	0.055	0.229

Table 2 AutoMAC of the POMs, computed between 3-nodes modes and 2-nodes and 4-nodes global modes for the case $Fr = 0$.

mode	nodes	$f_n^{POD}[Hz]$	δ [%]
1	2	7.3	1.19
5	3	22.3	2.02
7	4	34.7	1.41

Table 3 Modal damping of the segmented model in wet condition at $Fr = 0$.

The modal damping was evaluated by analyzing the modal coordinates associated to the identified modes. In particular the logarithmic decrement method was applied to the auto-correlation functions of the modal coordinates, obtaining a percentage modal damping as shown in Tab. 3. This technique allows then to obtain an estimation of the damping variation with the forward speed, as shown in Fig. 6, that is not easy to be obtained theoretically.

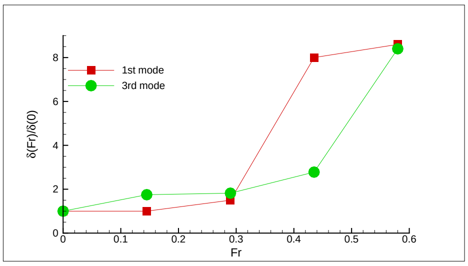

Fig. 6 Variation of damping with the Froude number in irregular sea.

REFERENCES

[1] R. Brincker, Ventura C.E., and P. Andersen, *"Why Output-Only Modal Testing is a Desirable Tool for a Wide Range of Practical Applications, "* XXI IMAC, 3-6/Feb., Orlando (FL) - USA, pp. 265-272, 2003.

[2] Karhunen, K., "Under lineare methoden in der wahrscheinlichkeitsrechnung", *Annals of Academic Science Fennicae Series, A 1, Math. Phys.*, Vol. 37(2), 1946.

[3] Lumley, J. L., "Stochastic tools in turbulence", Academic Press, New York, 1970.

[4] Kerschen, G., Golinval, J. C., Vakakis, A. F., Bergman, L. A. "The method of proper orthogonal decomposition for dynamical characterization and order reduction of mechanical systems: an overview", *Nonlinear Dynamics*, Vol. 41, pp. 147-169, 2005.

[5] Feeny, B. F., Kappagantu, R., "On the physical interpretation of proper orthogonal modes in vibrations", *Journal of Sound and Vibration*, Vol. 211(4), pp. 607-616, 1998.

[6] Dessi, D. and Mariani, R. "Analysis and prediction of slamming-induced loads of a high-speed monohull in regular waves," Journal of Ship Research, Vol. 52(1), pp. 71–88, 2008